Corresponding author:

Mr. Tymofii Tereshchenko, M.Sc.

Norwegian University of Science and Technology (NTNU)

Department of Energy and Process Engineering

Kolbjørn Hejes vei 1d

NO-7491 Trondheim

Norway

Phone: +4773598381

Mob: +4792553322

E-mail: tymofii.tereshchenko@ntnu.no

Implementation of CCPP for energy supply of future building stock

Nomenclature:

$f\ (-)$ – load factor, average heat load during heating season

$f_0\ (-)$ – load factor at the beginning of a heating season

$k\ (-)$ – radiator-type coefficient

$n\ (h)$ – operation hours of CCPP

$P_{comp,i}\ (GWh)$ – power production in CCPP with outdoor compensation temperature control

$P_{const,i}\ (GWh)$ – power production in CCPP with constant temperature control

$\dot{Q}_h^d\ (kW)$ – design value of the heat load

$\dot{Q}_h\ (kW)$ – heat rate

T_{ex}^d (°C) – design outdoor temperature

T_{ex} (°C) – outdoor temperature

T_{in} (°C) – indoor temperature in the building

T_r (°C) – return temperature in the DH network

T_s (°C) – supply temperature in the DH network

T_1 (°C) – supply temperature to DH system

T_2 (°C) – return temperature from DH system

T_{2d} (°C) – DH design temperature in return line

T_3 (°C) – supply temperature to hydronic heating system

T_{3d} (°C) – DH design temperature in supply line

u_m $(-)$ – mixing coefficient

τ (h) – duration of heating season

τ_i (h) – the ith value of heating hours

ΔT (°C) – temperature difference between supply and return lines in DH system

1. Introduction

Biomass Combined Heat and Power (CHP) plants are often seen as an efficient way to reduce greenhouse gas emissions due to their very low CO_2 emissions [1, 2]. The centralized production of the two energy types leads to greater efficiency in energy conversion and better emission control [3].

Bioethanol, or ethanol derived from biomass, has been recognized as a potential alternative to petroleum based transportation fossil fuels [4]. Among biofuels, bioethanol is the most widely used for transportation on a global basis and is consumed both as an individual fuel and in blends with gasoline [5]. Bioethanol can be produced from sugars, starch, and lignocellulosic biomass, of which the latter is often considered the most sustainable option as it

offers the possibility of reducing CO_2 emissions from transportation without influencing fuel prices and food prices directly [6]. Primary energy use from renewables in combination with CHP systems can lead to a significant reduction in CO_2 emissions. The CHP plants based on combined cycle technology, Combined Cycle Power Plants (CCPPs), reach a higher average fuel utilization of about 80%. The CCPP can achieve primary energy savings of between 9% and 20% and CO_2 emissions reductions in the same range. Renewable driven CCPP, in comparison with the carbon-intensive fossil fuel technology, achieves significantly higher emissions reductions [7].

The aim of this study was to investigate the operation of an ethanol-based CCPP, under changeable heat demand profiles, together with the possibilities of lowering temperature levels in a DH system. Due to strict energy requirements on new building constructions, energy units connected to supply DH systems, such as CCPPs, can demonstrate significant fluctuations in performance indicators. This is especially relevant because of the low energy buildings that are already connected, or will be connected, to the DH in the future. Due to low annual heat demand and high heat demand peaks during extreme outdoor conditions for such buildings, more insight needs to be devoted to this problem of the operation of CCPPs. Since the aim of this work was to analyze the performance of a CCPP at different loads and temperatures, a brief overview on building load trends and temperatures in DH is given in the following text.

1.1 Issues in estimating duration curve for future building areas

The estimation of heat demands is a complex task, especially for large-scale systems involving many heat consumers and consumer types [8]. There are many parameters, which could have an effect on heat load prediction in a DH system. Different authors implemented algorithms based on yearly observations for heat load prediction. Werner in [9] described a model based on physical theory. Different additive elements, for example wind speed and global radiation, were

added to the heat load model. Aronsson in [10] created a model which was based on Werner's work but with improvements. He formed the groups that shared the total heat demand load in a DH system. Arvaston in [11] concluded that outdoor temperature together with the social behavior of the customers has the greatest effect on heat demand, while different additive elements investigated by mentioned researches play a secondary role. Gadd and Werner in [12] mentioned that heat load can be split into social and physical components. Heat loads that depend on temperature difference and level of insulation belong to physical heat load. Distribution heat losses caused by pipe insulation can also be included in this category.

Retrofit of a DH system can affect heat load variation, since physical components such as pipe insulation or distribution pipes play an important role in the overall heat balance of a DH system. As mentioned in [13], typical relative heat losses in ordinary DH systems are 8 – 15% in Western and Northern Europe. The corresponding level is about 15 – 12% in Eastern Europe. Errors and deviations in customer substations and internal heating systems in buildings have a significant impact on the operation and load of heat supply plants. At the same time, our industrialized society always tries to automatize monitoring processes in different parts of DH systems. One of the future trends in the DH industry is smart systems. The smart DH will allow all the substations to be monitored automatically without enormous labor input. This can lead to smart load control and consequently to load decrease.

European Directive 2010/31/EU [14] stated that by the end of 2020 all new buildings should be nearly Zero-Energy Buildings (nZEB) and Member States should achieve cost-optimal levels by ensuring minimum energy performance requirements for buildings [15]. The change in the heat duration curve for the heat energy supply unit is inevitable with more buildings being connected to DH.

Currently, the entire building sector cannot consist of nZEB and passive houses. Therefore, the penetration of these buildings into the building stock will show an effect on use patterns in the future. The modernization of existing buildings has decreased the heat losses in EU countries, reducing the share of consumption of heat for space heating purposes [16]. This process has been already accomplished in Western Europe, leading to an increased effectivity in the heat supply for consumers and decreasing heat consumption throughout the year [17]. Werner and Olsson in [18] described the possibility of reducing the heat load variation for peak demand by using buildings connected to the DH system as a means of heat storage. In this study the authors assumed that the maximum time for heat storage discharge for different permitted changes in indoor temperature and different induced changes of the outdoor temperature should be 100 hours. Measurements were performed on different types of buildings (wooden, stone, tower blocks and old brick buildings). The conclusion was that the estimated time constants were often well above the assumed 100 hours for all types of buildings. Applying this strategy, an immediate increase in heat load during daytime temperature variation can be avoided for peak load energy units. The possibility of optimizing and reducing peak loads in DH systems, applying remote meters and control strategies, was described by Drysdale in [19].

However, it is not only the residential sector which can be connected to the DH system. With the increase in electricity prices, the industrial sector can shift from electrical heating to DH. Difs et al. in [20] investigated the possibility of integrating the industrial sector into existing DH systems. In this study the Method for Heat Load Analysis (MeLHA) was applied to 34 industries, located in various regions in Sweden and from different trade sectors. If industries use only DH services for space heating and hot tap water, then the integration effect will result in an additional load to base load plant, since the summer heat load is less than the plant’s minimum operating heat load. The conclusion from this study was that industrial processes can be

successfully integrated into the DH systems, with benefits to base load plants such as CHP systems.

Different heat load patterns from the customer side together with climate change and global warming [21, 22] can significantly decrease the profitability of energy supply units in DH systems. As stated in [23], a good practice consists of designing the CHP plant according to the minimum heat demand. However, in the case of DH networks, the minimum heat demand is very low and does not justify the installation of a CHP plant. Then the simple question emerges: How should DH companies react in the situation when the CHP unit is already installed, but the heat demand profile shows significant variation throughout the years? Therefore, the need for operation analysis f CHP systems with integrated DH systems and changeable heat demand profiles arises.

1.2 Trends in the temperature level of the DH system

From the beginning of the DH age in the world, three generations of DH distribution technology were developed [13]. In the earliest systems, steam was used as a heat carrier. Later on, water became the heat carrier. The materials used in the distribution system propagated different temperature and pressure levels. Nowadays, DH systems are predominantly built according to third generation principles. However, different countries have different requirements for supply and return temperatures in the DH system. In Sweden, for example, for many years the temperatures in hydronic systems were 80°C – 60°C, while in Germany, these values were greater and sometimes reached higher than 100°C in the supply line; in Eastern Europe it could even reach150°C. With the third generation of DH distribution technology, the reduction of distribution heat losses took place. Together with new building codes, these led to a decrease in supply and return temperatures in the DH network for areas with new types of buildings.

Considering different references [24-26], it can be noticed that for different types of buildings there are different requirements for temperature levels. Authors in [27] showed that even in the non-renovated houses in Denmark, it is enough to supply DH water at a temperature of 67°C. International studies [27-30] showed that there is an over-sizing of around 20 – 30% of DH systems and also of radiator systems, since designers want to be sure that the system provides enough heat. This can be the reason for further reductions in DH temperatures.

Future grids, with the fourth generation of DH technology, may use low-temperature heat distribution networks with normal distribution temperatures of 50°C – 20°C as an annual average [31].

However, in reality, it is not an easy task to implement the ideas regarding low temperature levels in DH systems, when combining them with heat energy units like CHP. Different publications devoted to low temperature DH mostly deal with future buildings and not the existing building stock which, due to the long lifetime of buildings, is expected to constitute the major part of the heat demand for many decades to come [31]. This means that without prepared infrastructure, it is almost impossible to bring ideas of low temperature DH to life. Different customers have different heat load characteristics and it is therefore sometimes rather complicated to satisfy all customers' demands with one temperature level lower than 80°C in the supply line of a DH system. One should also take into account the different types of structures being built during recent decades, as well as buildings at random stages of renovation [26, 27, 32, 33]. At the same time, a DH system should be competitive and cost-effective.

Nevertheless, the situation is different with the return temperature levels in the DH system. For certain types of CHP systems a high return temperature in the DH network could lead to a decrease in plant efficiency or it could be economically inefficient, depending on power and

heat outputs and the configuration of the plant. A higher return temperature results in higher heat losses, less energy stored in thermal storage, if that is used, and lower efficiency of heat generation. These facts make DH less attractive [34]. For these reasons, the authors considered that for DH systems connected to CHP units, a reduction in return water temperature should be implemented, leading to an increase in the temperature difference between supply and return lines. One of the ways to perform this is by the implementation of the “temperature cascading” [35] principle, suggested by researchers in [36]. This idea implies the connection of customers with low heat consumption to the return pipes, which is relevant for passive houses and nZEB buildings [37, 38]. Applying the temperature cascading principle and new substation schemes, as in [39], it is possible to obtain 20°C in the return line of a DH system and, with future improvements in buildings, insulation properties and distribution systems, even 15°C.

This paper is divided into the following sections: Section 2 introduces the methodology for the calculation of the temperature control strategy and heat duration curve in the DH system and process simulation of a CCPP; Section 3 describes the model and details of the process in the CCPP. Results of the analysis are discussed in Section 4. The final section outlines conclusions on the results from Section 4 and remarks on the possibilities for future work.

2. Methodology

The methodology presented in this section describes calculation techniques for the heat duration curve, an outdoor temperature compensation strategy within a DH system and a simulation method for the CCPP.

2.1 Estimation of heat duration curve

The heat duration curves used for estimating energy consumption in DH are individual for each DH system. The number of heating hours needed to supply customers depends on

geographical location, climatic conditions and outdoor temperature when the heating season begins, and building types connected to DH. Further, an issue with the construction of heat duration curve represents the major operation problem for DH companies. It is not fully possible to plan and predict heat supply to the customers and the fuel needed for the CCPP during an operation year [13].

Therefore, an analytical expression can be used for the calculation of the heat duration curve, applying the methodology presented in [40]. The final equation has the following representation:

$$\frac{\dot{Q}_h}{\dot{Q}_h^d} = 1 - (1 - f_0) \cdot \left(\frac{\tau_i}{\tau}\right)^{\frac{f - f_0}{1 - f}} \tag{1}$$

where f is a load factor (average relative heat load during the heating season) and f_0 is a load factor at the beginning of a heating season; τ and τ_i are duration of the heating season and the ith value of heating hours; $\dot{Q}_h$ is the heat rate, and $\dot{Q}_h^d$ is the design value of the heat rate for the minimum external temperature.

This expression is called Rossander's equation. As described in [40], it allows different heat duration curves to be built for different data sets.

In the current analysis, the authors assumed that the design external temperature is equal to -19°C, while the threshold temperature or beginning of the heating season is assumed when the outdoor temperature is equal to + 10°C. Rossander's analytical heat duration curve was built for these temperature conditions and is depicted in Fig. 5.

In this paper three duration curves are used for analysis. Two are based on measurements and one is the product of the authors' assumption. In order to justify selected duration curves, an analytical heat duration curve for predefined climatic conditions was used for comparison.

2.2 Supply water temperature control

There are different control options for supply and return temperatures in DH systems [13]. Such methods can be based on a constant supply temperature combined with local flow control, or a constant flow rate in combination with the control of supply temperature, or both. The control of the flow or supply temperature can be based on the feedback (indoor temperature) or the feed forward (outdoor temperature) control signal [41]. In this study, two control options were investigated: constant supply temperature from energy unit and outdoor temperature compensation.

In the case of the constant temperature control strategy, the supply temperature to the DH is set in the heat energy unit. Supply temperature remains constant during operation, while the control is performed by the adjustment of mass flow rate of water carrier to the customers. In the case of the outdoor temperature compensated curve, the highest supply temperature is reached at the design outdoor temperature. The return temperature is the result of the control strategy in customer substations and overall mixing of flows from all substations.

Outdoor temperature compensation in the DH network can be evaluated based on the methodology presented in [42]. In this methodology, the expected supply temperature in the DH network T_1 can be estimated as:

$$T_1 = (1 + u_m) \cdot T_3 - u_m \cdot T_2 \tag{2}$$

where T_2 and T_3 are expected DH return temperature and the expected supply temperature in the hydronic heating system in a building. u_m is the mixing coefficient. Then, the expected DH return temperature can be estimated as:

$$T_2 = T_3 - (T_{3d} - T_{2d}) \cdot \left(\frac{T_{in} - T_{ex}}{T_{in} - T_{ex}^d}\right) \tag{3}$$

where T_{ex}^{d}, T_{ex}, T_{in} are design outdoor temperature, outdoor temperature, and indoor temperature in the building, respectively. T_{2d} and T_{3d} are DH design temperatures in the return and supply lines, respectively.

The mixing coefficient can be evaluated as:

$$u_m = \frac{T_{3d} - T_1}{T_1 - T_2} \tag{4}$$

The expected supply temperature for the hydronic heating system can be estimated as:

$$T_3 = T_{in} + 0.5 \cdot (T_{3d} - T_{2d}) \cdot \frac{T_{in} - T_{ex}}{T_{in} - T_{ex}^{d}} + 0.5 \cdot (T_{3d} + T_{2d} - 2 \cdot T_{in}) \cdot \left(\frac{T_{in} - T_{ex}}{T_{in} - T_{ex}^{d}}\right)^{\frac{1}{1+k}} \tag{5}$$

Based on this methodology, Fig. 1 shows curves for the water temperatures in DH. The calculation was performed for a temperature level in the DH network of 100°C – 45°C.

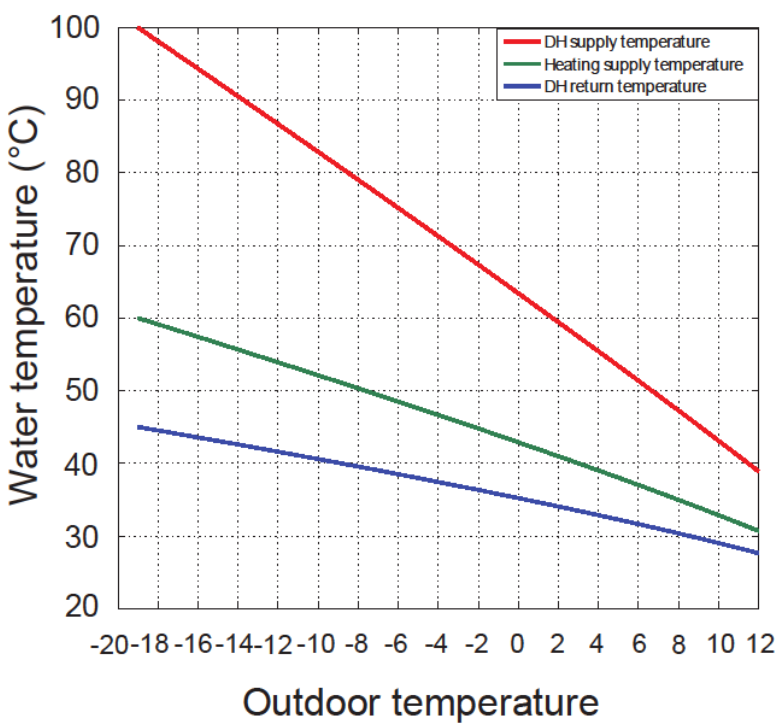

Fig. 1 Outdoor temperature compensated curves

2.3 CCPP simulation

In this paper heat and electricity production in the CCPP were simulated. The simulation process represents a transient calculation with a step size of one hour. The model of the CCPP was based on thermodynamic principles and performed in the Aspen HYSYS process simulation software. This commercial software is available for purchase. Different authors have performed analyses in this software and their publications validated the accuracy of the models being built in this software [43-46]. Data post processing was carried out using by MATLAB [47].

3. Case study

In this paper a small-scale DH system was studied, employing a CHP system with CCPP technology as an energy source for the DH system. The configuration of the CCPP system was an ethanol-driven gas turbine cycle (GTC), using exhaust heat recovery to drive a bottoming steam cycle (STC), with steam extraction for DH.

Ethanol-based CCPPs are well known, and different authors have performed studies on such systems [48-50]. The schematic layout of the system is presented in Fig. 2, and design parameters are summarized in Table 1.

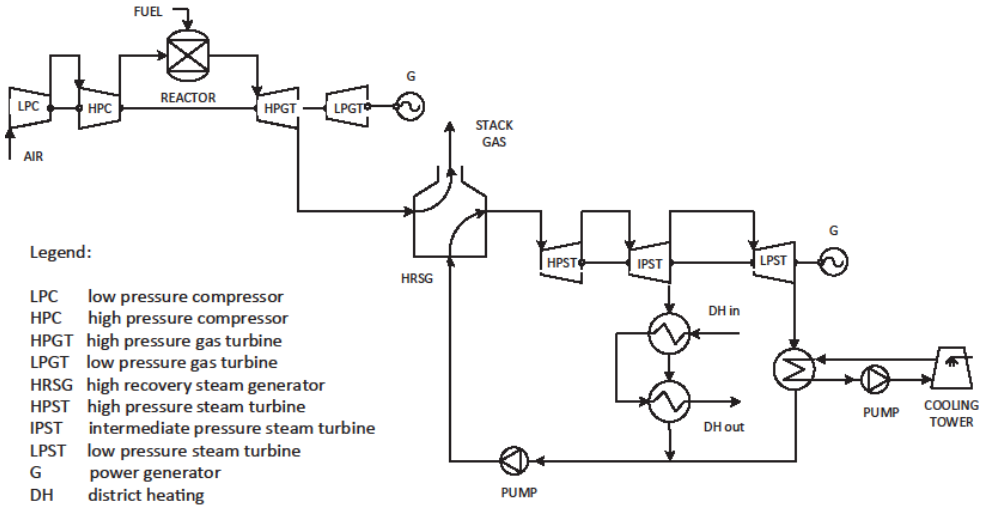

Fig. 2 Schematic of the CCPP

Table 1 Design point parameters of the CCPP

Parameter	Value
Ambient pressure	101 kPa
Air relative humidity	60%
Ambient air temperature	+15°C
Pump pressure	100 bar
Steam turbine inlet temperature	+540°C
Condensing pressure	0.05 bar
Air excess in air-fuel mixture	4.0
Fuel temperature	+15°C
Gas turbine adiabatic efficiency	0.9
Steam turbine adiabatic efficiency	0.9
Compressor adiabatic efficiency	0.9
Gas turbine inlet temperature	+1096°C
Supply temperature in DH system	+100°C
Return temperature in DH system	+45°C

The lower heating value (LHV) of the ethanol is 26.45 MJ/kg. The air and fuel were supplied to the reactor after a two-stage compression system. The low pressure compressor (LPC) provides pressure of 6 bar, while the high pressure compressor (HPC) compressed up to 15 bar; see Fig. 2. The air excess coefficient, α, was set to be 4.0 in the air-fuel mixture.

The GTC was represented by two units; one is a high pressure gas turbine (HPGT) and the other is a low pressure gas turbine (LPGT); see Fig. 2. The temperature of the flue gases entering the gas turbine was set 1096°C. The entering pressure of flue gases in the HPGT was 15 bar. The pressure before the LPGT was 6 bar. The leaving pressure was 1.5 bar, which is slightly higher than ambient conditions.

The high recovery steam generator (HRSG) was modeled as three stages of heat exchangers; see Fig. 2. These are an economizer, an evaporator and a superheater. The HRSG has one steam pressure level. The parameters of the live steam entering the steam cycle were: T =

540°C, p = 100 bar. The STC represented three units. The first was a high pressure steam turbine (HPST), the next was an intermediate pressure steam turbine (IPST), and the last was a low pressure steam turbine (LPST). The entering parameters of the working medium in the IPST were pressure of 12 bar and temperature 245°C. In the LPST, the steam condenses up to a pressure of 0.05 bar.

There is one extraction in the STC for DH purposes. The mass flow rate of water from the DH is satisfied with the heat exchange units. The DH system was fed from the IPST. The steam extraction occurred at a pressure of 10 bar.

Fig. 3 and Fig. 4 show changes in the plant performance due to change in air temperature, heat load and elevation. These curves were used for comparison with yearly operation values in the CCPP.

Fig. 3a shows the relative efficiency of the steam process, power process, and combined-cycle process as a function of ambient air temperature, while other ambient conditions and condenser pressure remain unchanged. The curves presented on the figures were based on a full DH load of 14 MW. The reference value of the ambient temperature was fixed at +15°C [51] for the design conditions. The reference elevation level is 0 m, which corresponds to ambient pressure of 1.013 bar. However, these values are changeable during the year and have a significant impact on plant performance.

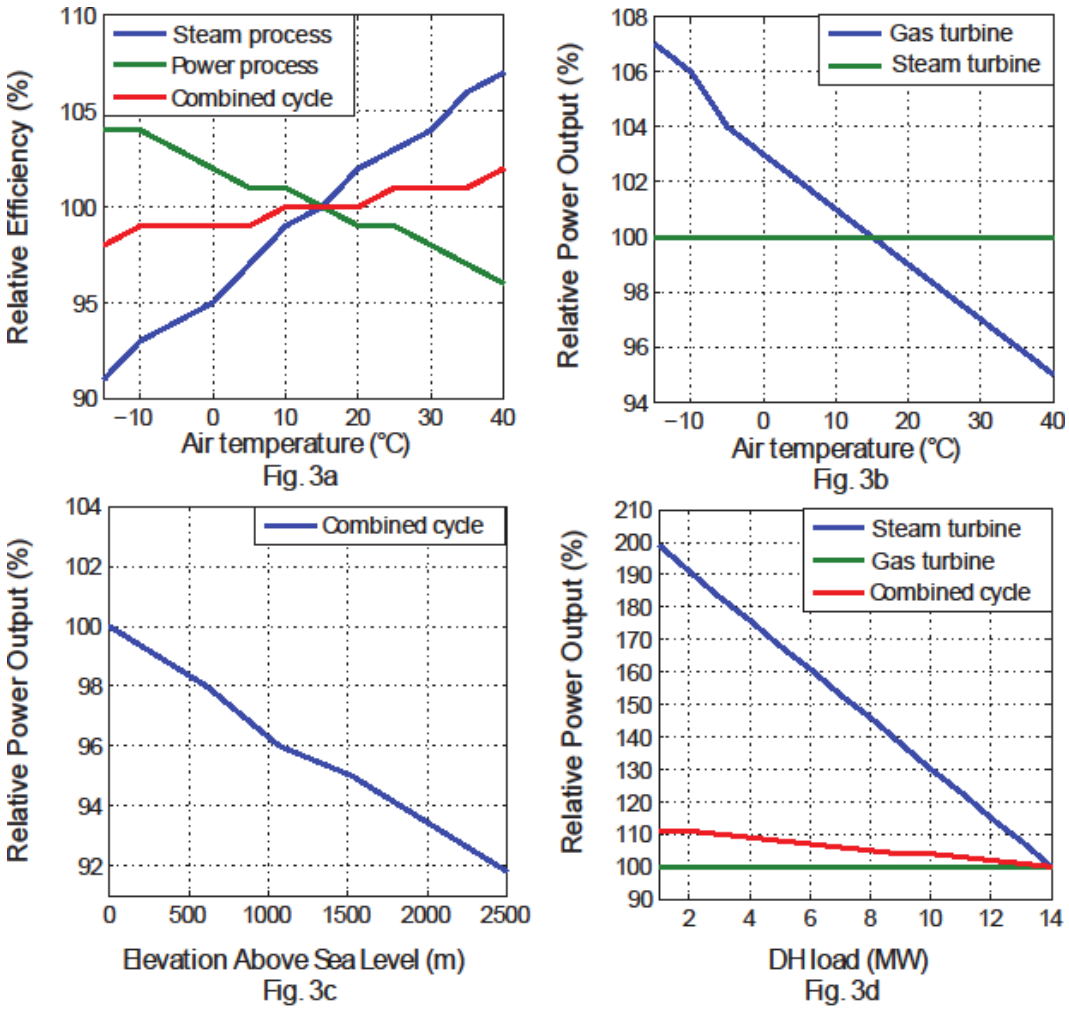

Fig. 3 CCPP design conditions

Fig. 3b shows the relative power output of a gas turbine and steam turbine in the CCPP. The relative power output of the steam turbine remains constant, since there is no change in the DH load. Fig. 3c presents the relative power output of the combined process due to the elevation above sea level. As can be seen, with an increase in elevation, the power output of the CCPP decreases due to the change in air density. Fig. 3d illustrates relative power output versus heat load in the DH system. The gas turbine cycle remains constant, since the change is only made to heat output in the range of 1 MW to 14 MW.

Finally, Fig. 4 presents the heat, power and energy efficiencies of the CCPP for different heat loads in the DH system.

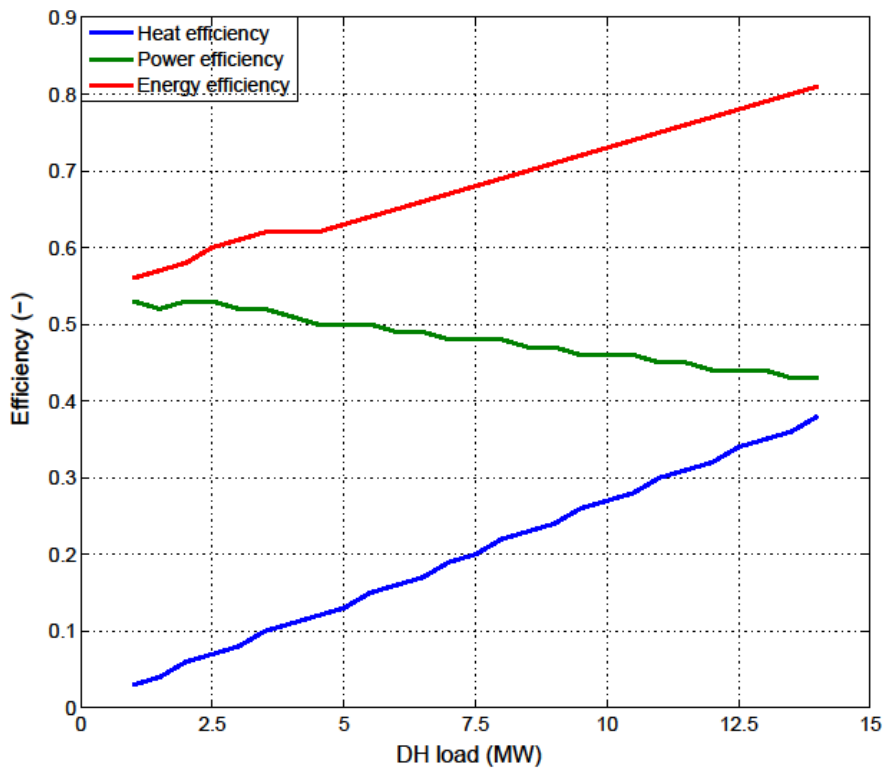

Fig. 4 Energy efficiencies of the analyzed CCPP

It is important to have design plant characteristics, as presented in Fig. 3 and Fig. 4. Such curves show the theoretical maximum and minimum of possible plant performance. However, these values are given for a certain reference point as previously discussed). In reality, when CHP plants operate under changeable seasonal heat loads, these parameters are far from the design point. The comparison with yearly operation values will shed light on the issue of variation in heat load profiles.

In this study, three heat demand profiles were considered to illustrate the heat use in the DH system. The analyzed duration curves are depicted in Fig. 5.

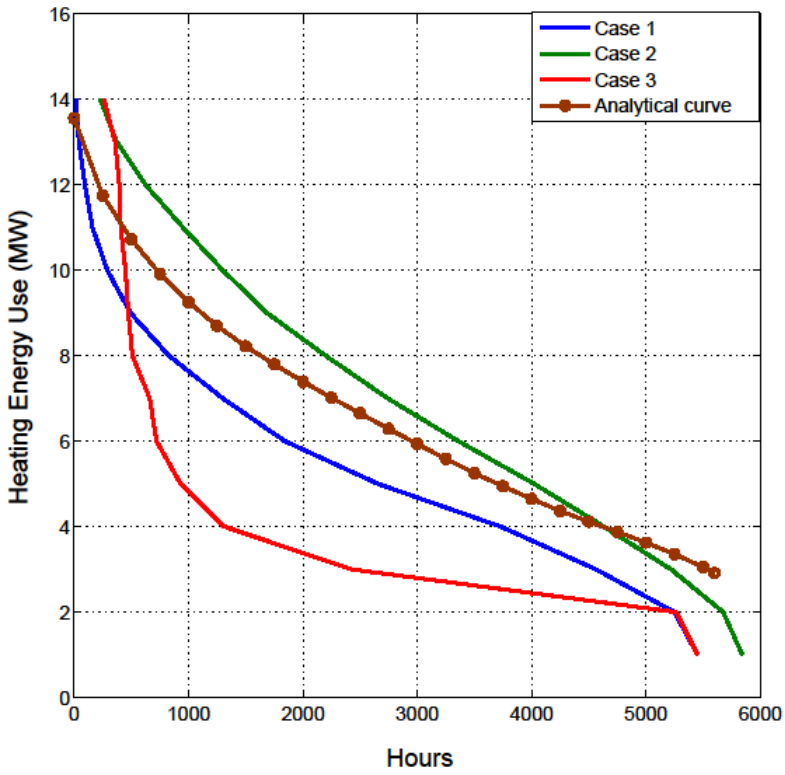

Fig. 5 Heat duration curve

Case 1 presents the heat duration curve during a regular year in the analyzed location and is used as a reference year. Case 2 presents the heat duration curve under a higher occupancy level and lower outdoor temperature. The heat duration curves in Case 1 and Case 2 are the result of measurements, which were carried out on the university campus. Case 3 represents the situation for future energy consumption, taking into account newly-built passive houses and nZEB with low heat energy use throughout the year and high peaks during the winter time. Case 3 is the result of an assumption and is represented by a decrease in heating energy use of almost 30% in comparison with the reference year. The heat load characteristics of the analyzed cases are summarized in Table 2.

Table 2 Heat load characteristics

	Rossander's	Case 1	Case 2	Case 3

	curve			
Heating energy use (GWh)	37.21	24.36	36.43	17.18
Average DH load (MW)	6.64	4.47	6.22	3.15
Difference in average DH load in comparison with the reference year (Case 1)	48.5%	-	39.2%	29.5%
Value of heat load at a maximum heating hours' frequency	-	4 MW	5 MW	2 MW

From Fig. 5 and Table 2, it can be seen that the analytical duration curve has the highest values of calculated heating energy use and average DH load. At the same time, the analytical curve gave values close to Case 2, which represents the scenario of higher occupancy and lower outdoor temperature. Rossander's equation was developed in the twentieth century, when climatic conditions were more severe and the length of the heating season was longer. Hence, the analytical curve shows the maximum possible heat energy use for the analyzed region. Later on, with the development of building codes and new energy policies, the heat energy use in buildings decreased. This is the situation presented by Case 1, where the value of heating energy use in the analytical duration curve is more than twice that of Case 3. This is reasonable, since nowadays there is a tendency to reduce as much as possible the energy consumption of all new building types. Moreover, future building stock cannot show higher energy consumption profiles. As can be noticed from Fig. 5 and Table 2, there is a tendency towards a reduction of heating energy use in building stock. This observation is very important, since heat energy units should be capable of withstanding the heat load decrease coming from customers.

Since the aim of this study was to analyze how the CCPP could be implemented for future building areas, a range of different supply and return temperatures was considered.

The temperature levels were chosen based on the review of the DH generations. A detailed explanation about the choice of temperature levels is provided in Section 1.2 of this paper. Taking into account different studies, conclusions, and the recommendations from these studies about temperature levels in DH systems, the temperatures presented in Table 3 were studied.

Table 3 Analyzed temperature levels in DH network

Explanation	Supply temperature in DH network Ts (°C)	Return temperature in DH network Tr (°C)
2nd Generation of distribution technology with medium return temperature	100	45
2nd Generation of distribution technology with low return temperature	100	30
2nd Generation of distribution technology with ultra-low return temperature	100	15
3rd Generation of distribution technology with medium return temperature	90	45
3rd Generation of distribution technology with low return temperature	90	30
3rd Generation of distribution technology with ultra-low return temperature	90	15
3rd Generation of distribution technology with medium return temperature	80	45
3rd Generation of distribution technology with low return temperature	80	30
3rd Generation of distribution technology with ultra-low return temperature	80	15

4. Results and discussion

4.1 Energy conversion in CCPP under different heat loads

Power productions for two temperature control strategies in the DH system are shown in Fig. 6. The shortcut “const” shows values for constant temperature control, while “comp” shows values for outdoor temperature compensated control.

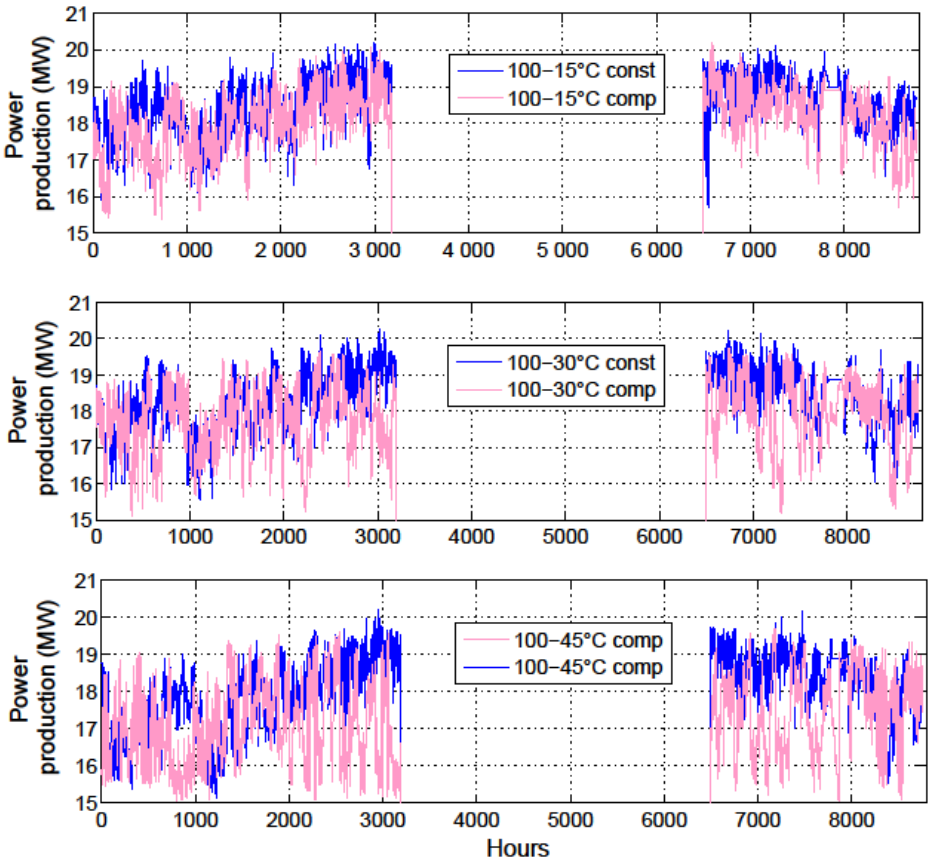

Fig. 6 Power production in the CCPP, for different control strategies and return temperatures in the DH system

In Fig. 6 it can be seen that the difference in power production of the CCPP, due to changes in control strategies with different supply and return temperatures, was not significant. Therefore, due to the enormous computational time needed for CCPP simulation over the entire year under two control strategies and at different temperature levels, the authors decided to focus only on the most relevant control option. For this reason, in order to identify the difference in the CCPP power production, the relative deviations between obtained results were calculated as:

$$\Delta P = \frac{1}{n} \cdot \sum_{i=1}^{n} \frac{\left(P_{comp,i} - P_{const,i}\right)}{P_{const,i}} \tag{6}$$

where $\boldsymbol{P_{const,i}}$ and $\boldsymbol{P_{comp,i}}$ are the values of power production in the CCPP with constant temperature control and outdoor temperature compensation strategies at time step $\boldsymbol{i}$. $\boldsymbol{n}$ is the number of operation hours of the CCPP.

Fig. 7 represents the relative deviation between the power productions in the CCPP for two different control strategies, with respect to the constant control strategy.

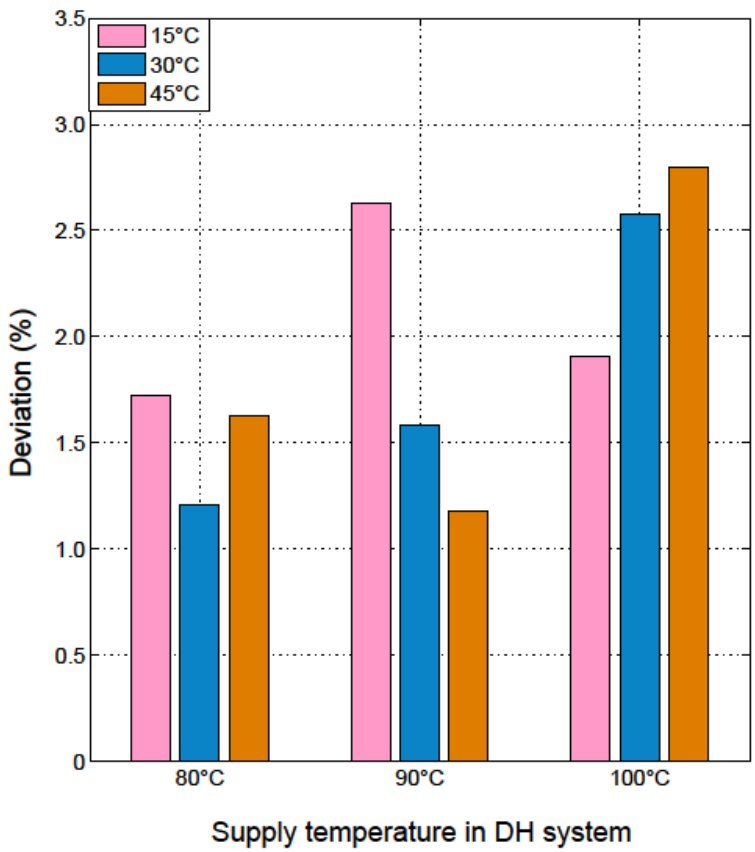

Fig. 7 Average deviation between two data sets

The difference between power productions for different temperature levels in DH systems is relatively small, under 3%, as shown in Fig. 7. The smallest deviation occurred in the temperature range of 80°C – 30°C, while the largest in 100°C – 45°C.

Due to different control strategies applied in the DH system, the annual amount of generated electricity in the CCPP also differs. Fig. 8 presents the annual power production for two strategies and different temperatures.

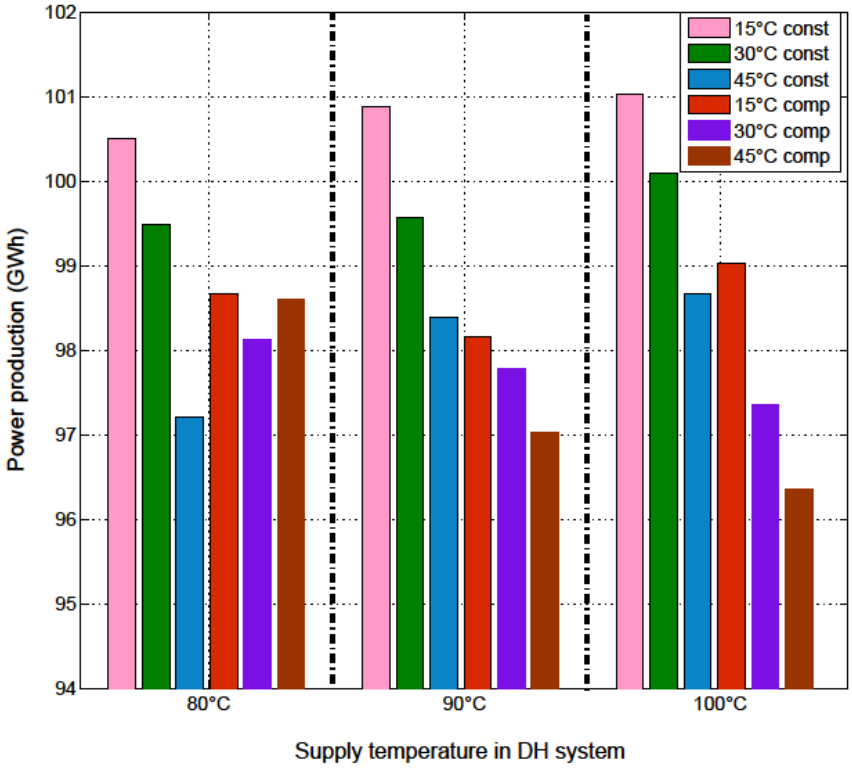

Fig. 8 Comparison of yearly power production in the CCPP for different supply and return temperatures and two control strategies in the DH system

Due to different control strategies, the yearly difference for the temperature range of 80°C – 30°C was 1.35 GWh and for 100°C – 45°C this value was 4.31 GWh of produced electricity.

For constant temperature control, the power production increases with the increase in supply temperature in the DH system for the same return temperature, while for temperature compensated control, the power production decreases with the increase in supply temperature in the DH system; see Fig. 8. Therefore, the lowest deviation between control strategies was found for the temperature level of 80°C – 30°C, while the largest was for 100°C – 45°C; see Fig. 7.

Fig. 8 reveals the fact that power production in the CCPP is sensitive to change in supply temperature in the DH system and also to the difference in change in temperature between supply and return lines. The greater the temperature difference in the DH, the more power is produced, regardless of which temperature control option is used.

Due to the relatively small difference in power production in the CCPP between the two control strategies applied in the DH system, see Fig. 7 and Fig. 8, in the further analysis only the constant supply temperature strategy was analyzed. Therefore, all future results are related to the constant supply temperature strategy.

In the current study three cases of heat energy use were analyzed. All analyzed cases have different characteristics, as shown in Fig. 5 and Table 2. One additional and very important characteristic used for description of heat energy use is the frequency diagram. It shows the frequency of heat load hours in the DH system throughout the operational year.

The heat load frequency diagram for analyzed cases of DH load is depicted in Fig. 9.

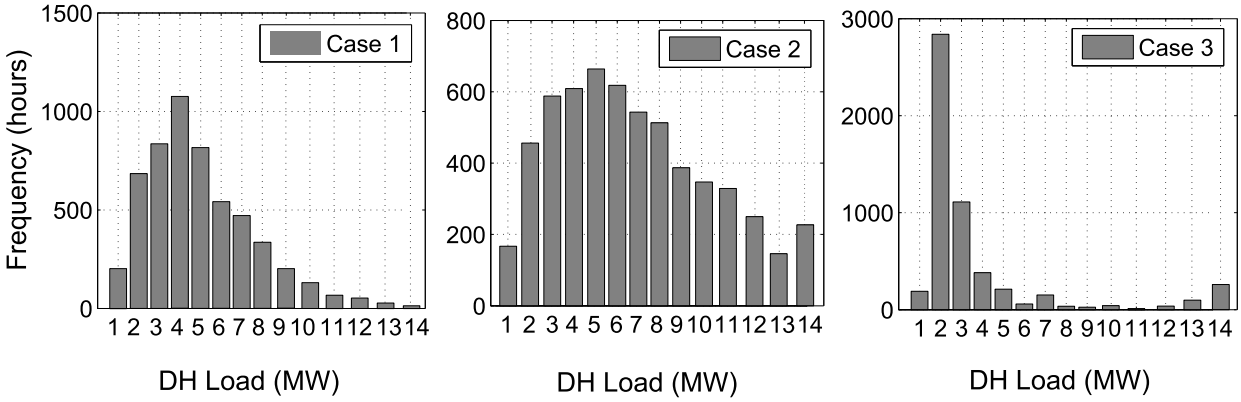

Fig. 9 Frequency of occurrence of heat load hours in DH system

In Fig. 9, it can be seen that Case 1 had maximum heating hours' frequency at 4 MW of DH load; further, with the increase in DH load, the heating hours' frequency decreased. In Case 2 the heating hours were evenly distributed throughout the load interval, while Case 3 showed a

pattern, which did not follow either Case1 or Case 2. Case 3 had maximum heating hours at 2 MW of DH load, while the rest of the DH load is sporadically distributed. The information depicted in Fig. 9 was very useful and could help to explain the simulation results.

Fig. 10 represents annual power production under different load profiles and temperature levels applied in the DH system.

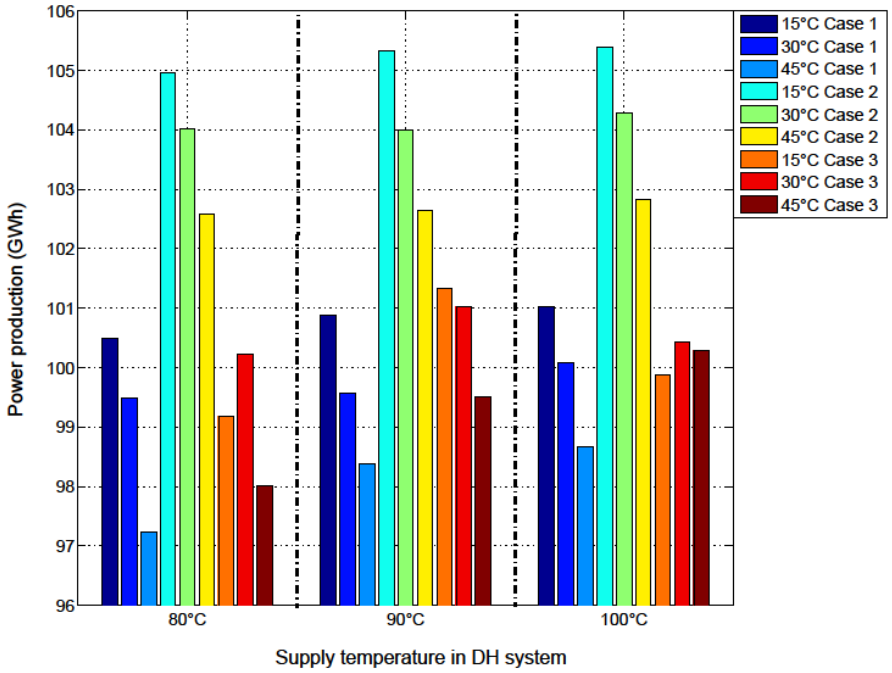

Fig. 10 Power production in the CCPP throughout the year

As can be seen from Fig. 9 and Fig. 10, Case 2 has a uniform distribution of heating hours between DH load, which resulted in higher power production in comparison with Cases 1 and 3. Further, a different trend was observed for the power production for Case 3 due to a change in the temperature levels; see Fig. 10. Different amounts of generated electricity during the year for Cases 1 – 3 could be explained by the different variation of heat load in the DH system.

For the supply temperature of 90°C, power production was decreased due to a decrease in the return temperature from 45°C to 15°C. However, in situations where the supply temperature was equal to 80°C and 100°C, the trend was different. For Case 3, the difference in power

production for the supply temperature of 100°C was negligible for all return temperatures, while for 80°C the highest value was obtained for a return temperature of 30°C. Further, the highest power production was obtained for the temperature level of 100°C – 15°C in Cases 1 and 2, indicating that the greatest temperature difference induced high power production. In the case of an increase in DH return temperature, the internal vapor pressure of the heat exchanger also increases. This phenomenon can cause steam pressure ascension, and the high steam energy is used for more heat output [52].

Fig. 11 shows heat efficiency in the analyzed CCPP depending on frequency of heat load hours in the DH system. Fig. 11 shows minimum, maximum, and mean values of heat efficiency for the analyzed scenarios.

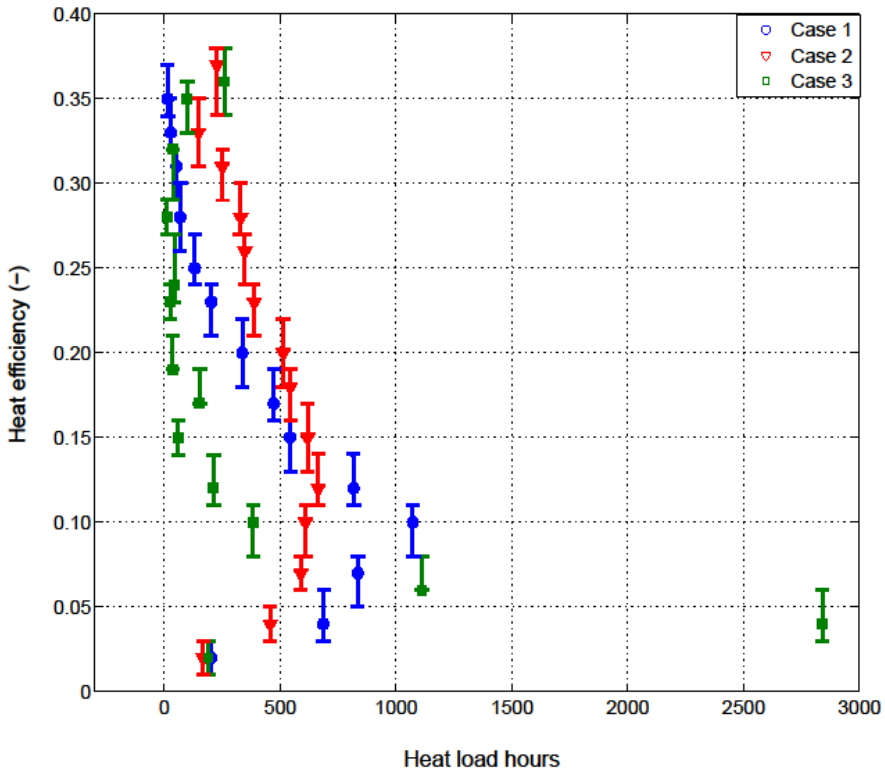

Fig. 11 Heat efficiency in the CCPP

Despite the fact that, in Case 3 there is the highest number of hours (2840) with the heat load of 2 MW, see Fig. 9, the heat efficiency of the CCPP is quite low. The highest heat

efficiency is found for the maximum heat load of 14 MW for all cases. The higher the DH load, the higher the plant capacity utilization and heat efficiency.

4.2 CCPP performance under different load and temperature levels

Fig. 12 presents average system performance characteristics for the analyzed CCPP, such as power efficiency, heat efficiency, and energy efficiency.

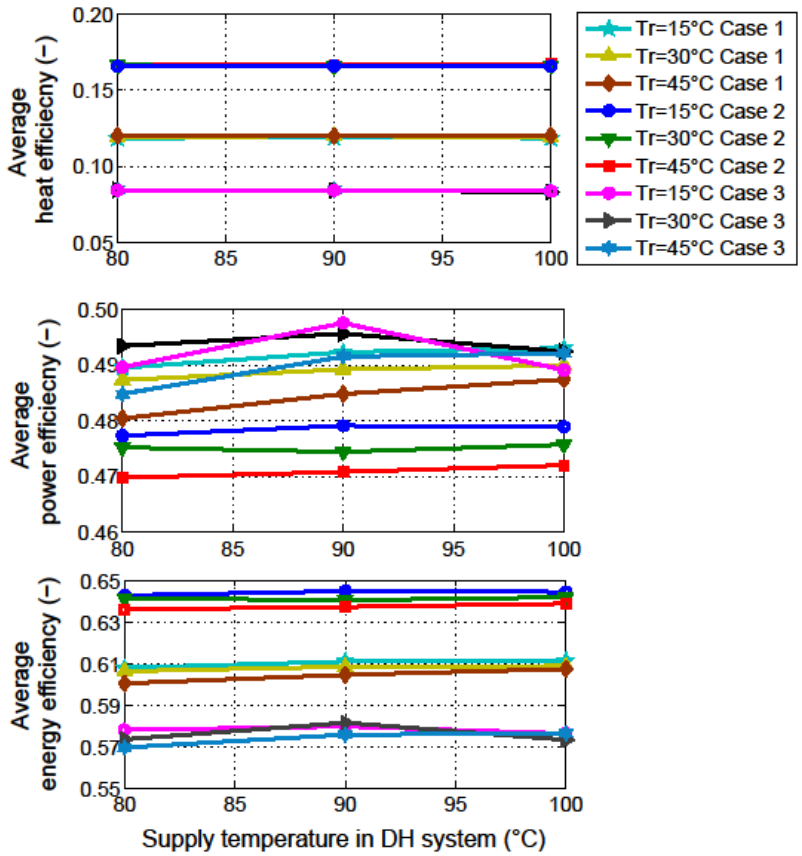

Fig. 12 Average heat, power, and energy efficiencies

Fig. 12 reveals that the results of average efficiencies in the CCPP varied among cases due to different load distribution. The calculated efficiencies were highly dependent on the DH heat load distribution. Fig. 12 shows that uniform distribution of heat load resulted in better plant operation throughout the year. The average heat efficiency for Case 2 is higher than for Cases 1 and 3. However, for different levels of supply and return temperatures, for all cases the change in

power efficiency and energy efficiencies was in the range of 1 – 2%, which is quite small. The maximum average energy efficiency was in the range of 57 – 65% for all cases. The obtained operation values were rather different from the design conditions; see Fig. 3 and Fig. 4. This observation indicated that plant was poorly loaded by the DH system throughout the year. This information should be considered while running the CCPP with the DH system.

Fig. 13 shows the change in power efficiency and DH load for Case 2 due to different heat load and different supply and return temperatures. Further, variations in the energy efficiencies are also shown. The figure shows minimum, mean, and maximum values obtained during simulations for corresponding heat loads.

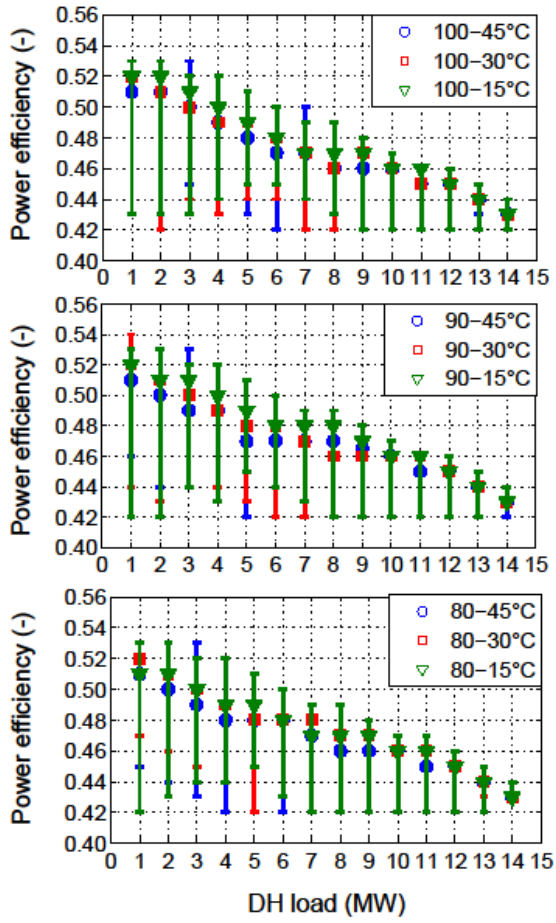

Fig. 13 Power efficiency for Case 2

Recalling Fig. 9, for Case 2, the highest number of heating hours occurred for the load equal to 5 MW, corresponding to 664 hours during the operation year, while the minimum of heating hours occurred at 13 MW (146 hours). The mean power efficiency for the DH load of 13 MW was equal to 0.44. This value was the same for all analyzed temperature levels. For the 5 MW of DH load, the mean power efficiency was in the range of 0.47 to 0.49, depending on temperature level used in the DH system. The diagram shows that power efficiency was sensitive to temperature difference in the DH system: the higher the temperature difference the higher the power efficiency.

Fig. 14 shows the distribution of the energy efficiency throughout the analyzed DH load interval for Case 2.

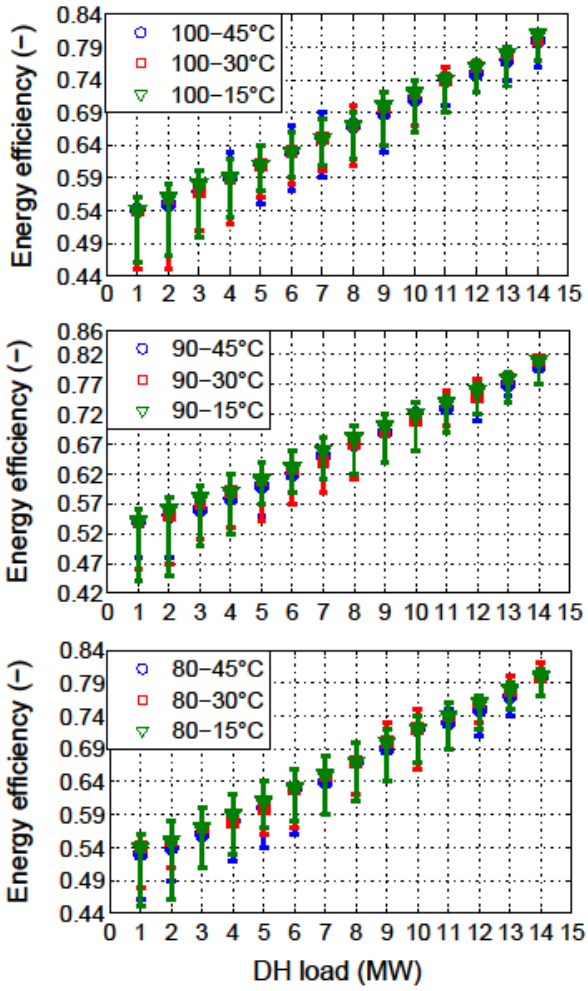

Fig. 14 Energy efficiency of the CCPP for Case 2

For the DH load of 5 MW, the energy efficiency was 0.60 – 0.61. Meanwhile, for the 13-MW DH load, the energy efficiency showed a value of 0.77 – 0.78, depending on different temperature levels in the DH system. Fig. 14 reveals that the difference in energy efficiencies was negligible for separate DH loads and analyzed temperature levels within subplots. However, in the case of continuous hour-by-hour operation of the CCPP, the deviation in energy efficiency is in the range of 2 – 10% between minimum and maximum values. This can be explained by rapid change of DH load, which results in an immediate response in fuel input and power production within the CCPP.

Of special interest is Case 3, since it reflects one of the possible scenarios in the future when the low energy buildings will share a certain part of the building stock. Low heating energy use makes such buildings unattractive for supply by large heat production units. This is the main drawback that heat production units must be capable of overcoming. Fig. 15 represents power efficiency for Case 3.

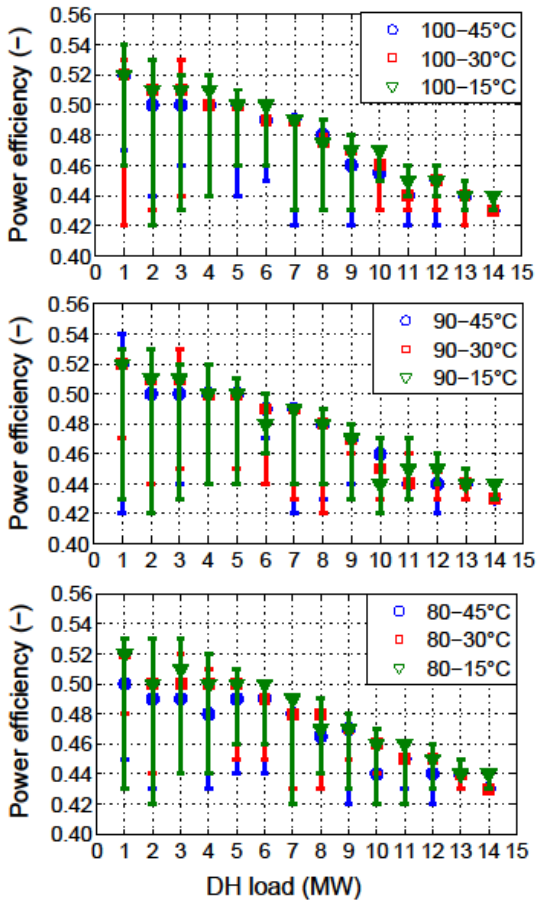

Fig. 15 Power efficiency for Case 3

The power efficiency for 11 MW of DH load was 0.45 for supply temperature of 80°C and return temperatures of 30°C and 45°C, while for 15°C this value was 0.46. For supply temperatures of 90°C and 100°C and corresponding return temperatures of 45°C and 30°C, the power efficiency was 0.44, while for 15°C this value was 0.45. The analysis showed the value of

power efficiency equal to 0.5 for 2 MW of DH load, with supply temperatures of 100°C and 90°C and return of 45°C. For the same level of supply temperatures and for 30°C and 15°C of return temperatures, the power efficiency increased by 2%. This indicated that temperature difference had a positive influence on power production within the STC. For a supply temperature of 80°C, the maximum power efficiencies of 0.5 were obtained for return temperatures of 30°C and 15°C. For 45°C, the power efficiency decreased by 2% and constituted 0.49; see Fig. 15. Further, Fig. 16 presents results on energy efficiency for Case 3.

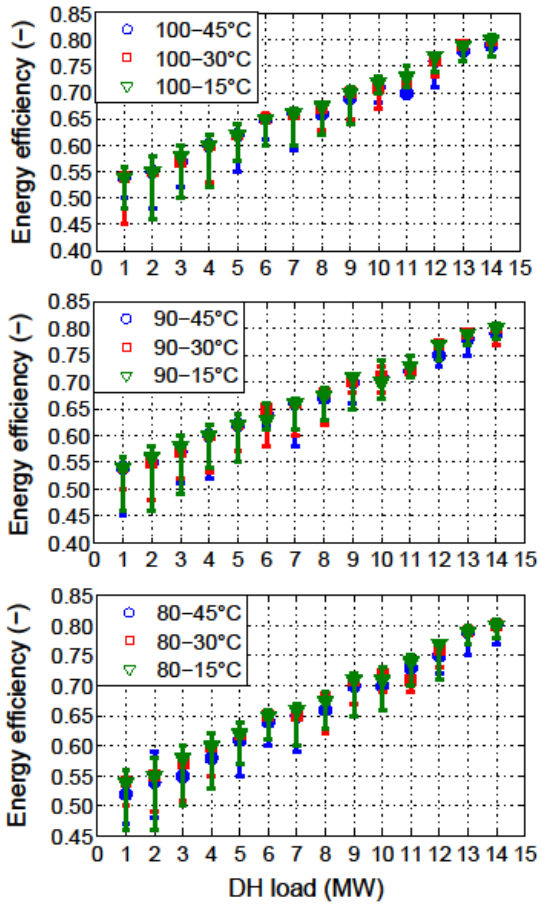

Fig. 16 Energy efficiency for Case 3

The deviations between mean values of energy efficiencies in analyzed DH load range were higher in comparison with Case 2, with respect to temperature levels in the DH system. For

11 MW of DH load and supply temperature of 100°C, the change in return temperature from 45°C to 30°C and then 15°C, resulted in 0.70, 0.72 and 0.73 of energy efficiency. For a supply temperature of 90°C, these values were in the range of 0.75 – 0.77. However, for 2 MW of the DH load and supply temperature of 100°C, the energy efficiency was equal to 0.55 for all return temperatures. For a supply temperature of 90°C, results showed a value of 0.55 for return temperatures of 45°C and 30°C and 0.56 for 15°C. For a supply temperature of 80°C and a return of 45°C, the energy efficiency was 0.54, while for 30°C and 15°C it increased and constituted 0.56; see Fig. 16.

The difference in mean values of power efficiency and energy efficiency between cases was not very large. This can be seen from Fig. 13, Fig. 14, Fig. 15, and Fig. 16. The deviation between minimum and maximum values of efficiencies varied from 2% to 10% depending on heat load rate. Meanwhile, the CCPP is sensitive to change in the DH load, especially if a long operation period is considered. The main conclusion that can be drawn is that it is beneficial to have a high heat load, while running the CCPP.

The values found in Fig. 13, Fig. 14, Fig. 15, and Fig. 16 are different in comparison with Fig. 3 and Fig. 4. One of the reasons is that design values were given at the maximum DH load and fixed reference point. In reality, it is quite complicated to run a CCPP based on full DH load due to variable heat load characteristics and high seasonal variations. Further, different elevations above sea level, ambient temperature and air pressure cause adjustments to plant operation.

4.3 Fuel use

Finally, Fig. 17 represents the fuel input within the analyzed CCPP.

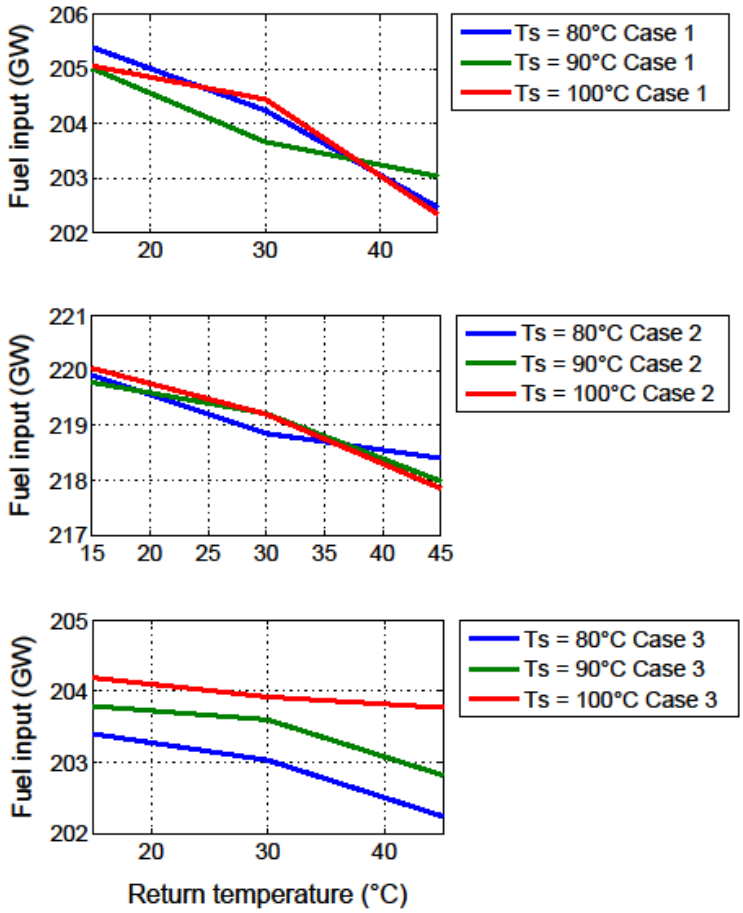

Fig. 17 Amount of fuel input in the CCPP

It can be seen that the reduction in return temperature shows a negative tendency in terms of fuel use. Cases 1 and 2 showed a gradual reduction in fuel input when the return temperatures increased. With the increase of temperature difference in the DH system, the fuel use increased; see Fig. 17. This happens because more energy input was required to heat up water in the DH system per 1K. However, for Case 3, the fuel energy input did not follow uniform increase with respect to temperature level used. This could be explained by rapid change in the DH load in the CCPP. Further, the load factor given in Equation (7) shows plant capacity utilization in terms of heating energy production. The load factor is the ratio of average load to the maximum load in the supply system [53].

$$\text{Load factor} = \frac{Average\ load}{Maximum\ load} = \frac{Energy\ consumed\ during\ a\ period}{Maximum\ demand \cdot utilization\ time} \quad (7)$$

Table 4 gives the values of the load factor for the analyzed cases.

Table 4 Heat load factor for analyzed cases

	Heat load factor (-)
Case 1	0.32
Case 2	0.45
Case 3	0.23

From Table 4 it can be seen that the load factor for Case 3 is the lowest. This indicates that the plant operates sporadically following the heat load during an operation year. The higher the load factor the cheaper the heat energy for the customer. In reality, it is very difficult to achieve a high load factor due to variable load characteristics from year to year.

The analysis of different temperature levels applied in the DH system indicated that the energy efficiency had negligible variation due to temperature levels in the DH system when running the CCPP. The reason for this is the high power production that takes place in the GTC. The analysis found that heat load distribution plays a crucial role in plant performance operation. Low heat load distribution leads to poor overall plant performance indicators. This gives incentives to run the plant for power production only. For this reason, when there is a need to select the DH supply and return temperatures for higher electricity production, the most effective method is to choose lower DH supply and return temperatures. Nevertheless, if we cannot change both of them, lowering the supply temperature is of more benefit [52].

Based on this study, it was concluded that it was rather difficult to operate a CCPP connected to low-energy building stock. Such buildings should be supplied from low temperature energy sources specially designed for this purpose. However, when high-grade heat is required,

the CCPP can be used to produce additional heating energy. This means that the CCPP is suitable for high-density heat areas, while it operates poorly in low heat density areas. For future building stock, it means that the CCPP could be successfully implemented if the areas were grouped at one place, rather than spread over a large area.

The information depicted within the different plots in this study could be used as a tool for plant behavior prediction if the further reduction of supply temperature in the DH network is considered.

5. Conclusion

In this paper, the performance of the ethanol-based CHP with CCPP technology was investigated in the DH system. The focus was on different temperature levels which could occur in today's and near-future DH systems. The two different temperature control strategies in the DH system were analyzed to estimate the effects on plant operation. Three possible scenarios of the DH load and different supply and return temperatures in the DH system were considered.

The results showed that the power production in the CCPP was not influenced significantly by the supply temperature control. The change in the power production was between 1.2% and 2.8%. Therefore, the focus in the study was on the constant supply temperature in the DH system.

The analysis of the change in DH load showed that average heat efficiency was highest for the uniform distribution load and lowest for very non-uniform load. The average power efficiency was dependent on different temperature levels in the supply and return lines of the DH system. The results showed that the highest power efficiency was obtained for the temperature levels of 100°C – 15°C and the lowest for 80°C – 45°C, for Case 1 and Case 2. This indicated that a large temperature difference between the supply and return lines of the DH system resulted

in higher power production in the CCPP. The results found that decrease in supply temperature had a low impact on energy efficiency. However, decreasing supply temperature to the DH system can lead to an increase in the service pipeline's lifetime, which is beneficial for the DH system. Another important conclusion is that the CCPP performance indicators are highly dependent on the heat load distribution in the DH system during the year. When DH load distribution had a uniform pattern throughout the operation year, as in Case 2, this resulted in better plant performance in comparison with Case 3. In the case of non-uniform heat load distribution, as in Case 3, plant performance was poor, indicating that the plant was poorly loaded. The results on load factor confirmed that fact, showing that in Case 2 the best possible heat load pattern for CCPP operation was obtained, while Case 3 represented the worst possible situation. However, in the current CCPP, GT technology was employed, which utilized the benefits of the low DH load by increasing power production. Analysis of all the CCPP performance indicators versus the DH load showed negligible variation for all the temperature levels applied in the DH system. The difference was in the range of 2 – 3% between cases. The change in the overall fuel energy input showed that fuel use increases with increase in temperature difference between supply and return lines in the DH system.

The results obtained in this study point out an inevitable decrease in plant profitability while operating the CCPP under low and non-uniform heat demand profiles. This observation provides incentives to shut down the heat supply to DH systems and run CCPP at full load, producing as much electricity as possible. Low energy building stock should be connected to specially designed low-grade temperature sources under a prepared infrastructure. However, CCPP could be used if low energy buildings were located close to each other to increase the heat density. The CCPP could also be used during the peak energy demand. This will have a positive

result on plant operation, since the CCPP will operate on its maximum heat load output, increasing its performance indicators.

The results obtained in this study can be used by designers of CHP systems, operators of DH systems, and legislators.

References:

[1] Lund H, Möller B, Mathiesen BV, Dyrelund A. The role of district heating in future renewable energy systems. Energy, 2010; 35(3): 1381-1390.

[2] Varun, Bhat IK, Prakash R. LCA of renewable energy for electricity generation systems – A review. Renewable and Sustainable Energy Reviews, 2009; 13(5): 1067-1073.

[3] Barelli L, Bidini G, Pinchi EM. Implementation of a cogenerative district heating system: Dimensioning of the production plant. Energy and Buildings, 2007; 39(6): 658-664.

[4] Govindaswamy S, Vane LM. Kinetics of growth and ethanol production on different carbon substrates using genetically engineered xylose-fermenting yeast. Bioresource Technology, 2007; 98(3): 677-685.

[5] Balat M. Production of bioethanol from lignocellulosic materials via the biochemical pathway: A review. Energy Conversion and Management, 2011; 52(2): 858-875.

[6] Gassner M, Maréchal F. Increasing efficiency of fuel ethanol production from lignocellulosic biomass by process integration. Energy & Fuels, 2013; 27(4): 2107-2115.

[7] Westner G, Madlener R. The impact of modified EU ETS allocation principles on the economics of CHP-based district heating systems. Journal of Cleaner Production, 2012; 20(1): 47-60.

[8] Heller AJ. Heat-load modelling for large systems. Applied Energy, 2002; 72(1): 371-387.

[9] Werner S. The heat load in district heating systems. Doctoral thesis. Department of Energy Conversion, Chalmers University of Technology, Gothenburg, Sweden; 1984.

[10] Aronsson S. Fjärrvärmekunders värme - och effektbehov—analys baserad på mätresultat från femtio byggnader. [Heat load of buildings supplied by district heating.] Doctoral thesis. Department of Building Services Engineering, Chalmers University of Technology, Gothenburg, Sweden; 1996.

[11] Arvaston L. Stochastic modelling and operational optimization in district heating system. Doctoral thesis. Mathematical Statistics, Lund University, Lund, Sweden; 2001.

[12] Gadd H, Werner S. Daily heat load variations in Swedish district heating systems. Applied Energy, 2013; 106(0): 47-55.

[13] Frederiksen S, Werner S. District heating and cooling. Studentlitteratur; Lund, Sweden, 2013, 586 p.

[14] EU. Directive 2010/31/EU of the European parliament and of the council - on the energy performance of buildings. Brussels: The European Parliament and the Council, 2010.

[15] Panão O, Marta JN, Rebelo MP, Camelo SML. How low should be the energy required by a nearly Zero-Energy Building? The load/generation energy balance of Mediterranean housing. Energy and Buildings, 2013; 61(0): 161-171.

[16] Ziębik A, Gładysz P. Optimal coefficient of the share of cogeneration in district heating systems. Energy, 2012; 45(1): 220-227.

[17] Gilijamse W, Boonstra ME. Energy efficiency in new houses. Heat demand reduction versus cogeneration? Energy and Buildings, 1995; 23(1): 49-62.

[18] Werner S, Olsson Ingvardson LC. Building mass used as short term heat storage, in The 11th International Symposium on District Heating and Cooling; 2008, Reykjavik, Iceland.

[19] Drysdale A. Optimized district heating systems using remote heat meter communication and control. IEA DHC Annex IV Report 2002:s7: DTI Taastrup, 2003.

[20] Difs K, Danestig M, Trygg L. Increased use of district heating in industrial processes – Impacts on heat load duration. Applied Energy, 2009; 86(11): 2327-2334.

[21] Berger T, Amann C, Formayer H, Korjenic A, Pospischal B, Neururer C, Smutny R. Impacts of climate change upon cooling and heating energy demand of office buildings in Vienna, Austria. Energy and Buildings, 2014; 80(0): 517-530.

[22] Wang H, Chen Q. Impact of climate change heating and cooling energy use in buildings in the United States. Energy and Buildings, 2014; 82(0): 428-436.

[23] Sartor K, Quoilin S, Dewallef P. Simulation and optimization of a CHP biomass plant and district heating network. Applied Energy, 2014; 130: 474–483.

[24] Swedish District Heating Association - Svensk Fjärrvärme. Available from: http://www.svenskfjarrvarme.se/ [Accessed 17th February 2015].

[25] Skagestad B, Mildenstein P. District heating and cooling connection hand-book, in: R&D Programme on District Heating and Cooling. International Energy Agency, 2002., Available from: http://www.districtenergy.org/assets/CDEA/Best-Practice/IEA-District-Heating-and-Cooling-Connection-Handbook.pdf [Accessed 17th February 2015].

[26] Hamada Y, Nakamura M, Ochifuji K, Yokoyama S, Nagano K. Development of a database of low energy homes around the world and analyses of their trends. Renewable Energy, 2003; 28(2):321-328.

[27] Brand M, Svendsen S. Renewable-based low-temperature district heating for existing buildings in various stages of refurbishment. Energy, 2013; 62(0): 311-319.

[28] Liao Z, Swainson M, Dexter AL. On the control of heating systems in the UK. Building and Environment, 2005; 40: 343–351.

[29] Peeters L, Van der Veken J, Hens H, Helsen L, D'haeseleer W. Control of heating systems in residential buildings: Current practice. Energy and Buildings, 2008; 40(8): 1446-1455.

[30] Trüschel A. Hydronic heating systems—the effect of design on system sensitivity. Doctoral thesis. Department of Building Services Engineering, Chalmers University of Technology, Gothenburg, Sweden; 2002.

[31] Lund H, Werner S, Wiltshire R, Svendsen S, Thorsen JE, Hvelplund F, Mathiesen BV. 4th Generation District Heating (4GDH). Energy, 2014; 1-11.

[32] Huang J, Henglin L, Gao T, Feng W, Chen Y, Zhou T. Thermal properties optimization of envelope in energy-saving renovation of existing public buildings. Energy and Buildings, 2014; 75(0): 504-510.

[33] Zvingilaite E. Modelling energy savings in the Danish building sector combined with internalisation of health related externalities in a heat and power system optimisation model. Energy Policy, 2013; 55(0): 57-72.

[34] Brandweiner O. Lower return temperatures within District heating Systems. A comparison of Danish and German District heating systems. MSc dissertation. Department of Development and Planning, University of Aalborg, Denmark; 2009.

[35] Rosa D, Boulter R, Church K, Svendsen S. District heating (DH) network design and operation toward a system-wide methodology for optimizing renewable energy solutions (SMORES) in Canada: A case study. Energy, 2012; 45(1): 960-974.

[36] Zinko H, Bohm B, Kristjansson H, Ottosson U, Rama, Miika & Sipila, Kachhwaha SS. District heating distribution in areas with low heat demand density, 2008, IEA DHC Annex VIII. International Energy Agency IEA District Heating and Cooling.

[37] Elsarrag E, Alhorr Y. Modelling the thermal energy demand of a Passive-House in the Gulf Region: The impact of thermal insulation. International Journal of Sustainable Built Environment, 2012; 1(1): 1-15.

[38] Rodriguez-Ubinas E, Sergio Rodriguez S, Karsten Voss K, Todorovic MS. Energy efficiency evaluation of zero energy houses. Energy and Buildings, 2014; 83(0): 23–35.

[39] Johansson PO, Jonshagen K, Genrup M, Lauenburg P, Wollerstrand J. Improved cooling of district heating water in substations by using alternative connection schemes. 22nd International Conference on Efficiency, Cost, Optimization, Simulation and Environmental Impact of Energy Systems; 2009; Foz do Iguaçu, Paraná, Brazil.

[40] Rujkin VY. Teplovue elektricheskie stancui (Combined heat and power plants in Russian). 3rd ed. Moskva: Energoatomizdat; 1987. 328 p.

[41] Lauenburg P, Wollerstrand J. Adaptive control of radiator systems for a lowest possible district heating return temperature. Energy and Buildings, 2014; 72(0): 132-140.

[42] Manyk VI, Kaplinsky YI, Hij EB. Nastroyka i ekspluataciya vodyanuh teplovuh setey (Adjustment and operation of district heating networks in Russian). 3rd ed. Moskva: Stroyizdat; 1988. 432p.

[43] Ong'iro A, Ugursal VI, Al Taweel AM, Lajeunesse G. Thermodynamic simulation and evaluation of a steam CHP plant using ASPEN Plus. Applied Thermal Engineering, 1996; 16(3): 263-271.

[44] Zheng L, Furimsky E. ASPEN simulation of cogeneration plants. Energy Conversion and Management, 2003; 44(11): 1845-1851.

[45] Ong'iro A, Ugursal VI, Al Taweel AM, Blamire DK. Simulation of combined cycle power plants using the ASPEN PLUS shell. Heat Recovery Systems and CHP, 1995; 15(2): 105-113.

[46] Aspen HYSYS. (Version 7.3) AspenTech. Available from: http://www.aspentech.com [Accessed 17th February 2015].

[47] MATLAB. (Version R2013a) MathWorks. Available from: http://www.mathworks.se [Accessed 17th February 2015].

[48] Zheng H, Kaliyan N, Morey RV. Aspen Plus simulation of biomass integrated gasification combined cycle systems at corn ethanol plants. Biomass and Bioenergy, 2013; 56(0): 197-210.

[49] Morey RV, Zheng H, Kaliyan N, Pham MV. Modelling of superheated steam drying for combined heat and power at a corn ethanol plant using Aspen Plus software. Biosystems Engineering, 2014; 119(0): 80-88.

[50] Starfelt F, Thorin E, Dotzauer E, Yan J. Performance evaluation of adding ethanol production into an existing combined heat and power plant. Bioresource Technology, 2010; 101(2): 613-618.

[51] International Standardization Organization. ISO2314:2009. Gas turbines - Acceptance tests. Switzerland; 2009.

[52] International Energy Agency. The potential for increased primary energy efficiency and reduced CO2 emissions by district heating and cooling: Method development and case studies.

By SP Technical Research Institute of Sweden, KDHC – Korea District Heating Technology Research Institute, SINTEF Energy Research Norway. ANNEX IX, 8DHC-11-01; 2011.

[53] Wadhwa CL. Generation, distribution and utilization of electrical energy. New York: Wiley; 1989. 367 p.